

Feedback between interacting transport channels

T. Brandes

Institut für Theoretische Physik, Hardenbergstr. 36, TU Berlin, D-10623 Berlin, Germany

(Dated: October 10, 2018)

A model for autonomous feedback control of particle transport through a large number of channels is introduced. Interactions among the particles can lead to a strong suppression of fluctuations in the particle number statistics. Within a mean-field type limit, the collective control mechanism becomes equivalent to a synchronization with an external clock. The diffusive spreading of the feedback signal across the channels shows scaling, can be quantified via the flow of information, and shows up, e.g., in the spectral function of the particle noise.

PACS numbers: 05.40.-a, 05.10.Gg, 05.60 -k

I. INTRODUCTION

Feedback loops are an interesting tool to modify and control the transport dynamics of systems, both classical and quantum [1–10]. Increasing efforts have been made recently to understand and quantify closed loop control schemes (e.g. in Maxwell demon, information tape or network models) from the perspective of thermodynamics, statistical mechanics and system-bath theories [11–27].

A key question here is how to design the feedback loop itself, i.e. whether to regard it as part of some active external measurement scheme, or ‘passively’ as an extended part of the system itself. This latter form of coherent control [28–33] is particularly appealing for quantum systems (also cf. [33] for coherent feedback control of quantum transport and further references), as it avoids the need to involve the measurement process. But also classically, a full microscopic understanding of feedback control requires the modeling of some form of interaction between the system and its controller.

It is this perspective from which we re-visit a feedback control scheme [34] of a stochastic process describing (source to drain) transport of particles, which in its simplest version describes a continuous, active modulation of transition rates conditioned upon the full counting statistics (FCS) [35], i.e. the statistics $p(n, t)$ of particle numbers n that have accumulated in a drain reservoir after a certain time t . In the new feedback model, this modulation is achieved in passive mode via interactions among particles in N coupled transport ‘channels’ that provide the feedback by making the individual transition rates in each channel dependent upon the (reservoir) state of the entire system.

The starting point in this paper thus is an infinite system of coupled Poissonian processes for the FCS obtained by adiabatic elimination of internal ‘connector’ degrees of freedom between source and drain reservoirs, cf. Fig. (1a). Detailed balance for the transition rates then already restricts the form of possible feedback models that can be obtained from microscopic interactions. Choosing a classical limit of weakly interacting uncharged fermions, we interpret the interaction-induced strong reduction of fluctuations as a ‘condensation’ in the space of reservoir

particle numbers. This is accompanied with an instantaneously increased flow of information between a given channel and the rest of the system. For periodic channel structures, Fourier analysis yields detailed predictions for the diffusion-like spreading of the autonomous feedback signal across the channels, which can be made visible in observables like the particle noise spectrum.

II. MODEL

Our model is defined by a d -dimensional lattice with N lattice sites \mathbf{R}_l , $l = 1, \dots, N$, each of which serves as a connector within a channel with particle flow from a source to a drain reservoir at rate γ_{l+} (‘forward’), and backwards from drain to source at rate γ_{l-} , cf. Fig. (1a). There is no direct transfer of particles between different channels, but the time-independent rates $\gamma_{l\pm} = \gamma_{l\pm}(\mathbf{n})$ are allowed to depend on the state $\mathbf{n} \equiv (n_1, \dots, n_N)^T$ of all the drain reservoirs. These are defined by the numbers $n_l \in \mathbb{Z}$ of additional particles in drain reservoir l , when counting starts at time $t = 0$.

The dynamics is described by a Markovian rate equation for the probability $p(\mathbf{n}, t)$ of the drain reservoirs to be in state \mathbf{n} at time t ,

$$\dot{p}(\mathbf{n}, t) = \sum_{\mathbf{n}'} [\Gamma(\mathbf{n}, \mathbf{n}')p(\mathbf{n}', t) - \Gamma(\mathbf{n}', \mathbf{n})p(\mathbf{n}, t)], \quad (1)$$

where $\Gamma(\mathbf{n}', \mathbf{n}) \equiv \sum_{l=1}^N \sum_{\pm} \gamma_{l\pm}(\mathbf{n}) \delta_{\mathbf{n}', \mathbf{n} \pm \mathbf{e}_l}$ with the Cartesian unit vector $\mathbf{e}_l = (0, \dots, 1, \dots, 0)^T$, such that we can write

$$\dot{p}(\mathbf{n}, t) = \sum_{l=1, \pm}^N [\gamma_{l\mp}(\mathbf{n} \pm \mathbf{e}_l)p(\mathbf{n} \pm \mathbf{e}_l, t) - \gamma_{l\mp}(\mathbf{n})p(\mathbf{n}, t)], \quad (2)$$

which makes the contributions from forward and backward jumps in the N channels explicit. As initial condition for $p(\mathbf{n}, t)$ we set $p(\mathbf{n}, 0) = \delta_{\mathbf{n}, 0}$.

The rate equation Eq. (2) can be generalized to the more complex situation where the N connectors between the source and drain reservoirs have themselves an internal structure, i.e. internal states (like in quantum

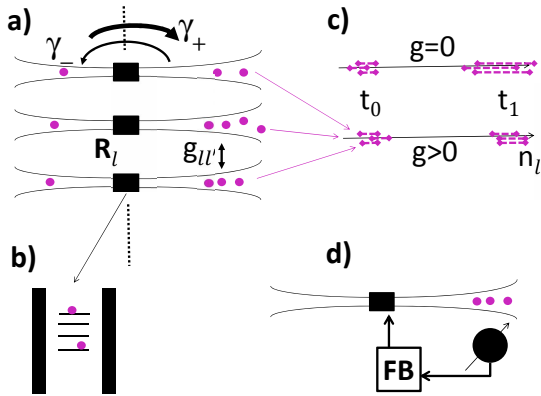


FIG. 1: (a) Particle transport between source and drain reservoirs at rates γ_{\pm} through connectors in channels at positions \mathbf{R}_l . (b) Connectors could have internal states. (c) Autonomous feedback via interactions ($g > 0$) among drain reservoirs reduces fluctuations of particle numbers n_l , represented as Brownian particles on a line. This is compared to the non-feedback case $g = 0$ during time evolution from t_0 to t_1 . (d) Active, non-autonomous measurement-based feedback for a single channel [34].

dots) that can be occupied by particles. It seems difficult to make progress then (apart from large-scale numerics), but on the other hand the above rate equation then can follow as an effective model via adiabatic elimination when time-scale separation is possible. For example, this is the case with one internal state connected to a source at a very fast rate and a drain at a very slow rate (not shown here). In all what follows, we will therefore work with Eq. (2) as the starting point.

The rates $\gamma_{l\pm}(\mathbf{n})$ are the key elements in describing the interactions among the channels and the effective feedback mechanism created thereby, which is why we discuss them in quite some detail in the following.

A. Decoupled channels with time-dependent rates

In the simplest version of the feedback model, the rates have the time (t) and n -dependent form

$$\gamma_{l\pm}(\mathbf{n}) = f_{\pm}(I_l t - n_l), \quad (3)$$

where the function $f_{\pm}(x)$ describes a synchronization between the actual number n_l with an external reference $I_l t$ that grows linearly with time (‘clock’ with a fixed control current I_l). The form Eq. (3) then immediately reduces Eq. (2) to decoupled rate equations for the single-channel probabilities $p_1(n, t)$, cf. Eq. (A4) in Appendix A. Physically, this kind of feedback can be achieved via an instantaneous control, i.e. a modification of the rates ‘by hand’ in an active way by an external agent like an electronic circuit, cf. Fig. 1d).

For example, a linear modulation $f_{\pm}(x) = \gamma_{\pm}(1 \pm gx)$ with control parameter $0 < g \ll 1$ continuously compensates particle number fluctuations in that the forward rate γ_+ is decreased if there are too many particles as compared to a reference charge $I_l t$. The rate equation can then be solved exactly, and the main result [34] is a freezing of the single channel full counting statistics $p_1(n, t)$ at large times t around a mean $\langle n \rangle_t \propto t$. Quantitatively, the second cumulant follows from Eq. (2) as

$$\langle n^2 \rangle_t - \langle n \rangle_t^2 = \frac{1}{2g} \left(1 - e^{-2g(\gamma_+ + \gamma_-)t} \right), \quad (4)$$

which means that fluctuations are strongly suppressed for $g > 0$, which is schematically shown in Fig. 1c). In a similar way, expressions for higher cumulants [34] can be derived that all saturate at finite values $\propto 1/g$ at large times t .

B. Interacting channels

Alternatively, feedback occurs via the design of interactions among particles. In most of what follows we will be dealing with an autonomous form

$$\gamma_{l\pm}(\mathbf{n}) = \gamma_{\pm} \left[1 \pm \sum_{j=1}^N g_{lj} (n_j - n_l) \right], \quad (5)$$

which is parametrized by interaction matrix elements g_{lj} and which is linear in the n_l . The rates Eq. (5) are a generalization of the Eq. (3) in the following way: consider the simplest all-to-all coupling $g_{ij} = \frac{g}{N}$ for which the rates have the form $\gamma_{l\pm}(\mathbf{n}) = f_{\pm}(n_{\text{av}} - n_l)$, with the average $n_{\text{av}} \equiv (n_1 + \dots + n_N)/N$ and $f_{\pm}(x) = \gamma_{\pm}(1 \pm gx)$ as above. Now, for $N \rightarrow \infty$ the average n_{av} becomes a macroscopic variable, and neglecting the fluctuations of the latter against those of n_l one obtains the rates Eq. (3) with $I_l t = \langle n_{\text{av}} \rangle$, i.e. we recover the synchronization model in this mean-field limit (see Appendix A for some more details).

The rates Eq. (5) have a very intuitive form: the n_l -dependence leads to a dynamical compensation of particle number differences among the channels. If there are too many particles in the drain reservoir l (as compared to all the other drains $j \neq l$), the forward (backwards) rate for channel l is decreased (increased), and the other way round if there are too many particles in drain l . As we will show below, this compensation mechanism tends to suppress *fluctuations* of the drain reservoir particle numbers n_l also within each single channel l .

The rates Eq. (5) can potentially become negative (and the model unphysical) in the linear approximation; however, this is not really a problem as long as the interactions are sufficiently small. More importantly, with the g_{lj} as unspecified parameters, we have not yet addressed the issue of detailed balance between forward and backward rates so far.

C. Detailed balance

We therefore consider a dependence of $\gamma_{l\pm}(\mathbf{n}) \equiv r_l(\varepsilon_l(\mathbf{n}))$ on the energy differences $\varepsilon_l(\mathbf{n}) \equiv \Delta\mu_l + \Delta E_l(\mathbf{n})$, where $\Delta\mu_l \equiv \mu_{l,d} - \mu_{l,s}$ is the difference of the chemical drain and source potentials in channel l , and $\Delta E_l(\mathbf{n}) \equiv E(\mathbf{n} + \mathbf{e}_l) - E(\mathbf{n})$ with the energy $E(\mathbf{n})$ due to interactions among the particles in all drain channels. Correspondingly, $\gamma_{l-}(\mathbf{n} + \mathbf{e}_l) = r_l(-\varepsilon_l(\mathbf{n}))$, and detailed balance reads

$$\gamma_{l+}(\mathbf{n}) = \gamma_{l-}(\mathbf{n} + \mathbf{e}_l) e^{-\beta[\Delta\mu_l + \Delta E_l(\mathbf{n})]}, \quad (6)$$

where all the channels are kept at the same temperature $k_B T = \beta^{-1}$.

By expanding the rates $r_l(\varepsilon_l(\mathbf{n}))$ and the r.h.s. of Eq. (6) in the interaction energies $\Delta E_l(\mathbf{n})$, we find a linearization

$$\gamma_{l\pm}(\mathbf{n}) = \gamma_{l\pm} \times \left(1 + \frac{r'_l(\pm\Delta\mu_l)}{r_l(\pm\Delta\mu_l)} [E(\mathbf{n} \pm \mathbf{e}_l) - E(\mathbf{n})] \right) \quad (7)$$

with $\gamma_{l\pm} \equiv r_l(\pm\Delta\mu_l)$, which is consistent with detailed balance if $\Delta E_l(\mathbf{n})$ is sufficiently small.

We can be more specific in Eq. (5) if we model the particles as fermions that tunnel between a non-interacting (source) and an interacting (drain) region, similar to the orthodox model of Coulomb blockade for charged fermions (electrons) in metallic quantum dots [37]. In this case, the specific expression

$$r_l(\varepsilon) = r_l \frac{\varepsilon}{e^{\beta\varepsilon} - 1} \quad (8)$$

can be derived, where r_l is a parameter that depends on the (flat) density of states in source and drain reservoirs. The coefficient in the rate Eq. (7) then becomes $\frac{r'_l(\pm\Delta\mu_l)}{r_l(\pm\Delta\mu_l)} \approx -\beta/2$ provided $\beta|\Delta\mu_l| \ll 1$, in which case detailed balance is always fulfilled in lowest order in $\beta\Delta E_l(\mathbf{n})$ in Eq. (6). This also shows that in this expansion, we are dealing with rates in a high-temperature limit, where the particles essentially behave as classical objects and quantum statistics and quantum coherence plays no role. What we are left with as a key modeling parameter are the interactions among the particles.

D. Interaction form

In order to make analytical progress with Eq. (2), we further linearize the rates $\gamma_{l\pm}(\mathbf{n})$ in \mathbf{n} by assuming a quadratic dependence

$$E(\mathbf{n}) \equiv \frac{1}{2} \mathbf{n}^T U \mathbf{n} \quad (9)$$

with a symmetric $N \times N$ matrix U of interaction parameters whence Eq. (7) becomes

$$\gamma_{l\pm}(\mathbf{n}) = \gamma_{l\pm} \left[1 \mp \frac{\beta}{2} \mathbf{e}_l^T U \mathbf{n} \right], \quad (10)$$

where we neglected a constant, \mathbf{n} -independent term.

From Eq. (10) we recognize that we obtain the feedback form Eq. (5) with the identification

$$U_{lj} = \frac{2}{\beta} \left(\delta_{lj} \sum_{i=1}^N g_{li} - g_{lj} \right) \quad (11)$$

and homogeneous rates $\gamma_{l\pm} = \gamma_{\pm}$ independent of channel index l . For example, with $g_{lj} = \frac{g}{N}$ and a single interaction parameter $g > 0$, one has $U_{lj} = \frac{2}{\beta} g (\delta_{lj} - \frac{1}{N})$, which mimics a mean-field type repulsive interaction within the same channel $l = j$, and an attractive interaction between particles in different channels $l \neq j$, regardless of particle distance. The form Eq. (11) means that the interaction matrix U has a zero eigenvector $(1, 1, \dots, 1)^T$ such that

$$\sum_{j=1}^N U_{lj} = 0 \quad (12)$$

and the (repulsive) interaction strength U_{ll} within each channel l is cancelled by the sum of the remaining (attractive) interactions with all other channels j . Physically, such an interaction corresponds to a repulsive short-range and an attractive long-range, van-der-Waals like force between uncharged particles.

The choice of parameters in the interaction matrix U_{lj} in Eq. (9) is restricted to the particular form Eq. (11), because we demand a stationary particle current to flow through the channels, i.e. a situation where the average numbers n_l continue to grow linearly with time t .

We obtain the equation of motion for these averages $\langle n_l \rangle \equiv \sum_{\mathbf{n}} n_l p(\mathbf{n}, t)$ from Eq. (2) by summation over n_l , as

$$\frac{d}{dt} \langle n_l \rangle = \langle \gamma_{l+}(\mathbf{n}) - \gamma_{l-}(\mathbf{n}) \rangle \quad (13)$$

or $\frac{d}{dt} \langle \mathbf{n} \rangle = \Delta\gamma + (G^+ + G^-) \langle \mathbf{n} \rangle$, in matrix form with the matrix $G_{lj}^{\pm} \equiv -\frac{\beta}{2} \gamma_{l\pm} U_{lj}$ and the vector $\Delta\gamma_l = \gamma_{l+} - \gamma_{l-}$. For general U_{lj} , this equation has a fixed point with $\langle \mathbf{n} \rangle = -G^{-1} \Delta\gamma$ for invertible $G \equiv G^+ + G^-$. Here, however, we are interested in the opposite case where G (and thus U) is not regular but has a zero eigenvector $(1, 1, \dots, 1)^T$ leading to Eq. (12) and Eq. (11).

As an immediate consequence, we find the solution of Eq. (13)

$$\langle n_l \rangle = (\gamma_+ - \gamma_-) t, \quad (14)$$

i.e. a linear increase of the particle numbers in all channels regardless of the interaction strength.

III. FLUCTUATIONS

The average flow of particles has the rather trivial form Eq. (14) for the homogeneous case considered here and in the following, i.e. equivalence of all channels l with

translational invariance across the d -dimensional lattice of connectors between source and drain reservoirs. As in our previous work [34], we expect the feedback to drastically modify the full counting statistics of the particle numbers n_l . The most important object to quantify fluctuations then is the second cumulant. Higher cumulants are difficult to extract from Eq. (2), except for special cases as in [34], and we will therefore effectively evaluate only a Gaussian model for the fluctuations.

A. Second cumulant

We quantify the fluctuations by the correlation function

$$C_{ll'}(t) \equiv \langle n_l n_{l'} \rangle - \langle n_l \rangle \langle n_{l'} \rangle, \quad (15)$$

for which we obtain an equation of motion via Eq. (2). Multiplication of Eq. (2) with $(\mathbf{n}e_l)(\mathbf{n}e_{l'})$ and summation over \mathbf{n} yields $\frac{d}{dt}\langle n_l n_{l'} \rangle = \sum_{\pm} \langle \delta_{ll'} \gamma_{l\pm}(\mathbf{n}) \mp n_l \gamma_{l'\pm}(\mathbf{n}) + (l \leftrightarrow l') \rangle$, and for the homogeneous case with rates Eq. (5) we obtain

$$\frac{d}{dt} C_{ll'} = \gamma \left(\delta_{ll'} + \sum_{j=1}^N g_{lj} (C_{lj} - C_{ll'}) + l \leftrightarrow l' \right) \quad (16)$$

with the definition $\gamma \equiv \gamma_+ + \gamma_-$. We can now take advantage of the discrete translational invariance on the lattice $\{\mathbf{R}_l\}$ of channel connectors l by defining the Fourier decomposition $C_{ll'} = \frac{1}{N} \sum_{\mathbf{k}\mathbf{k}'} \hat{C}_{\mathbf{k}\mathbf{k}'} e^{-i\mathbf{k}\mathbf{R}_l + i\mathbf{k}'\mathbf{R}_{l'}}$ in reciprocal space for the correlation function and

$$g_{lj} = \frac{1}{N} \sum_{\mathbf{k}} e^{-i\mathbf{k}(\mathbf{R}_l - \mathbf{R}_j)} \hat{g}(\mathbf{k}) \quad (17)$$

for the interaction matrix elements in Eq. (5).

We solve Eq. (16) for an initially empty drain reservoirs with $C_{ll'}(0) = 0$,

$$C_{ll'}(t) = \frac{1}{N} \sum_{\mathbf{k}} e^{-i\mathbf{k}(\mathbf{R}_l - \mathbf{R}_{l'})} \sigma_{\mathbf{k}}(t), \quad (18)$$

with the definitions

$$\sigma_{\mathbf{k}}(t) \equiv \frac{\gamma}{\Gamma_{\mathbf{k}}} (1 - e^{-\Gamma_{\mathbf{k}} t}), \quad \Gamma_{\mathbf{k}} \equiv 2\gamma(\hat{g}(0) - \hat{g}(\mathbf{k})), \quad (19)$$

which are real quantities as we recognize from the representation $\hat{g}(\mathbf{k}) = \frac{1}{N} \sum_{ll'} e^{i\mathbf{k}(\mathbf{R}_l - \mathbf{R}_{l'})} g_{ll'}$ and the symmetry $g_{ll'} = g_{l'l}$.

Infinite range interaction. — We first evaluate the result Eq. (18) for the mean-field type model $g_{ij} = \frac{g}{N}$ in the interactions Eq. (11), which (simple as it is) already contains the essential ingredients of the feedback mechanism we try to analyse here.

Using $\hat{g}(\mathbf{k}) = \frac{g}{N^2} \sum_{ll'} e^{i\mathbf{k}(\mathbf{R}_l - \mathbf{R}_{l'})} = g\delta_{\mathbf{k},0}$, from Eq. (19) we obtain

$$\Gamma_{\mathbf{k} \neq 0} = 2g\gamma. \quad (20)$$

The $\mathbf{k} = 0$ contribution in the sum Eq. (18) is extracted with the limit $\Gamma_{\mathbf{k}=0} = 0$, and we have

$$C_{ll'}(t) = \frac{\gamma t}{N} + \left(\delta_{ll'} - \frac{1}{N} \right) \frac{1}{2g} (1 - e^{-2\gamma g t}), \quad (21)$$

where we used $\sum_{\mathbf{k} \neq 0} e^{-i\mathbf{k}(\mathbf{R}_l - \mathbf{R}_{l'})} = N\delta_{ll'} - 1$ for the second term.

The result Eq. (21) already captures one of the main ingredients of the feedback mechanism described by our model: at large times t , the fluctuations $C_{ll'}(t)$ increase linearly but are suppressed by a factor of $1/N$ as compared to the simple non-interacting case with the Poissonian fluctuations $\langle \delta n_l^2(t) \rangle = \gamma t$.

In the limit of a very large number of channels, for times such that $N \gg \gamma t \gg 1$ we obtain a freezing of the fluctuations towards the value $C_{ll'}(t) \rightarrow \delta_{ll'}/2g$. For the fluctuations within one channel, this becomes visible as a plateau at intermediate times in Fig. (2a), where we plot $C_{ll}(t)$ for various values of N .

In each channel l , a synchronization occurs where in the rates Eq. (5) the contributions from all the other channels can be replaced by a time-dependent average Eq. (3) with $I_l t = (\gamma_+ - \gamma_-)t$. This is in accordance [34] with the non-autonomous model Eq. (3), where we found a freezing of the entire full counting statistics around a moving mean value Eq. (14) at large times t , with a second cumulant Eq. (4) that co-incides with Eq. (21) for $N \rightarrow \infty$. In our mean-field model here, instead of synchronization with an external ‘clock’ current I_l , we have auto-synchronization between all channels. In Appendix A, we demonstrate the equivalence between the synchronization model Eq. (3) and the N -channel model with infinite range interactions in the mean field limit by deriving the equation of motion for the single channel probability $p_1(n, t)$.

Diffusion limit and scaling. — We now evaluate the result Eq. (18) in the opposite limit of short-range interactions g_{ij} , which has a more interesting dynamics as compared to the mean-field case above. We can evaluate the Fourier-matrix elements $\hat{g}(\mathbf{k})$ for nearest-neighbor interaction in Eq. (17),

$$g_{lj} = g\delta_{(lj)}, \quad g > 0. \quad (22)$$

For example, on an infinite lattice with lattice constant a in $d = 1$ dimension, we have $\hat{g}(k) = 2g \cos ka$.

The decay rates Eq. (19) acquire the form

$$\Gamma_{\mathbf{k}} = 2\gamma g a^2 \mathbf{k}^2, \quad |\mathbf{k}| \rightarrow 0 \quad (23)$$

in the continuum limit where the connector lattice constant a approaches zero. In the terminology of dynamical phase transitions, this corresponds to model-A dynamics [38, 39] due to the fact that the total particle number $N_{\text{tot}} \equiv \sum_l n_l$ in the drains grows with time and is not conserved.

The diffusive nature of the feedback dynamics is now clear from the second cumulant Eq. (18), the temporal

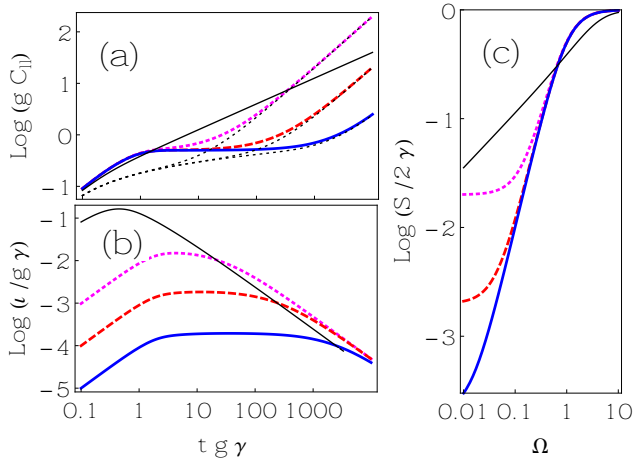


FIG. 2: (a) Diagonal second cumulant C_{ll} Eq. (21) multiplied with interaction parameter g and (b) information current $\iota_{l' \rightarrow 1}$, Eq. (40), as a function of time t multiplied with $g\gamma$. (c) Stationary diagonal noise spectrum ($l = l'$, Eq. (25)) as a function of scaled frequency $\Omega \equiv \omega/(g\gamma)$. Curves for infinite range interaction model Eq. (20) with channel numbers $N = 50$ (magenta dotted), $N = 500$ (red dashed), $N = 5000$ (blue thick line), diffusive approximation Eq. (23) in $d = 2$ dimensions with finite N in (a), and nearest neighbor model Eq. (22) in $d = 1$ dimension with $N \rightarrow \infty$ (thin black line).

derivative of which,

$$\dot{C}_{ll'}(t) = \frac{\gamma}{N} \sum_{\mathbf{k}} e^{-i\mathbf{k}(\mathbf{R}_l - \mathbf{R}_{l'})} e^{-2D\mathbf{k}^2 t}, \quad (24)$$

has the form of a d -dimensional diffusion propagator, where $D \equiv \gamma g a^2$ is an effective diffusion constant. Accordingly, we obtain the simple, d -dependent temporal and spatial (with respect to $|\mathbf{R}_l - \mathbf{R}_{l'}|$) scaling behavior of $C_{ll'}(t)$ characteristic of a critical dissipative Gaussian model [39] with dynamical critical exponent $z = 2$.

For any finite number N of channels, the integral approximation to the \mathbf{k} -sum Eq. (18) has a lower cutoff at the inverse system size $\propto N^{-1/d}$. With increasing d , at intermediate times $C_{ll}(t)$ develops a flat plateau as in the all-to-all coupling model Eq. (20), before the linear in t behaviour sets in at very large times. This is shown in Fig. (2a) for the diffusive model Eq. (23) in $d = 2$ (with the same values for N as in the all-to-all coupling model), and for the full nearest-neighbor interaction model Eq. (22) in $d = 1$ in the limit $N = \infty$, where $C_{ll}(t \rightarrow \infty) \propto t^{1/2}$.

B. Noise Spectrum

The above temporal fluctuations can be related to the fluctuations $\delta I_l(\tau) \equiv I_l(\tau) - \langle I_l \rangle$ of the particle currents $I_l(\tau)$ in a stationary situation, as quantified by the sym-

metrized noise spectrum

$$S_{ll'}(\omega) \equiv \int_{-\infty}^{\infty} d\tau e^{i\omega\tau} \langle \delta I_l(\tau) \delta I_{l'}(0) + \delta I_{l'}(\tau) \delta I_l(0) \rangle. \quad (25)$$

We use the MacDonald formula [40, 41] together with the regression theorem [42] to obtain the two-time correlation functions $\langle \delta n_l(t) \delta n_{l'}(t + \tau) \rangle$ for $t \rightarrow \infty$ (cf. Appendix C) and find

$$S_{ll'}(\omega) = 2 \frac{\gamma}{N} \left(1 + \omega^2 \sum_{\mathbf{k} \neq 0} \frac{\cos(\mathbf{k}(\mathbf{R}_l - \mathbf{R}_{l'}))}{\Gamma_{\mathbf{k}}^2/4 + \omega^2} \right). \quad (26)$$

We have evaluated Eq. (26) for the infinite range interaction model, Eq. (20), and for the nearest-neighbor interaction model Eq. (22) in $d = 1$ dimension. In both cases, the diagonal noise $l = l'$ is independent of the channel index l and displays scaling, i.e. a dependence on the dimensionless variable $\Omega \equiv \omega/(g\gamma)$ that in both cases contains the feedback strength parameter g ,

$$\frac{S_{\infty}}{2\gamma} = \frac{1}{N} + \frac{N-1}{N} \frac{\Omega^2}{1+\Omega^2} \quad (27)$$

$$\frac{S_{d=1}}{2\gamma} = \sqrt{\frac{1}{2} \left(\frac{1}{\sqrt{1+16/\Omega^2}} + \frac{1}{1+16/\Omega^2} \right)}. \quad (28)$$

The noise spectra in these two cases have the correct high-frequency (or zero feedback $g = 0$) Poissonian limit $S(\Omega \rightarrow \infty) = 2\gamma$, cf. Fig. (2c).

The opposite limit of zero frequency $\omega = 0$ corresponds to the Poissonian long-time $t \rightarrow \infty$ limit Eq. (21) at any finite N for S_{∞} , whereas the $N = \infty$ lattice model (nearest neighbor interaction) is determined by diffusive dynamics in d dimensions at small frequencies (that fails on short time- or large frequency scales),

$$\frac{S_d(\omega)}{2\gamma} = \frac{1}{2\sqrt{2}} \left(\frac{\omega}{g\gamma} \right)^{\frac{d}{2}}, \quad \omega \rightarrow 0, \quad (29)$$

which also follows from Eq. (23) with Eq. (26). The noise reduction at low frequencies highlights the strong suppression of fluctuations in each transport channel due to the feedback from all the other channels.

IV. HEAT AND INFORMATION

A. Condensation picture

The interaction-induced feedback mechanism among the channels leads to a ‘condensation’ of the system into a state $p(\mathbf{n}, t)$ where fluctuations of the particle numbers n_l are essentially suppressed at large times.

Without feedback, the addition of the N independent Poissonian processes (channels) in the *total* particle number $n_{\text{tot}} \equiv \frac{1}{N} \sum_l n_l$ (normalized by N) leads to

$\langle \delta n_{\text{tot}}(t)^2 \rangle = \gamma t/N$: the fluctuations of the macroscopic variable n_{tot} are reduced by a factor $1/N$ as compared to the fluctuations $\langle \delta n_l(t)^2 \rangle = \gamma t$ in the individual, ‘microscopic’ channel variables n_l .

In contrast, with feedback the microscopic fluctuations are reduced at large times t , $\langle \delta n_l(t)^2 \rangle \rightarrow \gamma t/N$, whereas the form Eq. (19) guarantees that the fluctuations of n_{tot} are not affected by the feedback: summation of Eq. (18) over l , use of $\frac{1}{N} \sum_{l,l'} e^{-i\mathbf{k}(\mathbf{R}_l - \mathbf{R}_{l'})} = N\delta_{\mathbf{k},0}$ and the limit $\Gamma_{\mathbf{k}=0} = 0$ again leads to $\langle \delta n_{\text{tot}}(t)^2 \rangle = \gamma t/N$, and the microscopic and macroscopic fluctuations are now of the same order.

This explains the scheme shown in Fig. (1c), where the channel variables n_l are (continuous) position coordinates x_l of a large cluster of N interacting Brownian particles on a line, with the cluster center-of-mass coordinate corresponding to $n_{\text{tot}}(t)$. The feedback (interactions) then condenses the (at time $t = 0$) ‘gas’ of initially independent particles into a tightly bound cluster, where fluctuations of *relative* distances between particles do not grow with time (as without feedback) but approach the fixed value obtained from Eq. (18) as

$$\langle (n_l - n_{l'})^2 \rangle_{t \rightarrow \infty} = \frac{2\gamma}{N} \sum_{\mathbf{k} \neq 0} \frac{1 - \cos(\mathbf{k}(\mathbf{R}_l - \mathbf{R}_{l'}))}{\Gamma_{\mathbf{k}}}. \quad (30)$$

B. Heat

Starting from initially empty drains, this condensation process is accompanied by an increase in interaction energy $E(\mathbf{n})$, Eq. (9), which has to be compensated by a flow of heat from the reservoirs that keep the drains at constant temperature and chemical potential all the time. Explicitly, a simple calculation leads to

$$\frac{d}{dt} \langle E(\mathbf{n}) \rangle_t = \frac{1}{2\beta} \sum_{\mathbf{k}} \Gamma_{\mathbf{k}} e^{-\Gamma_{\mathbf{k}} t}, \quad (31)$$

with the rates $\Gamma_{\mathbf{k}}$ defined in Eq. (19). By integration of Eq. (31), the quadratic interaction potential Eq. (9) thus leads to the equipartition $\langle E(\mathbf{n}) \rangle_{\infty} - \langle E(\mathbf{n}) \rangle_0 = \frac{1}{2} k_B T N$, i. e. an interaction energy $\frac{1}{2} k_B T$ stored in each channel.

At the same time, the constant current $I \equiv \gamma_+ - \gamma_- \geq 0$ of particles (cf. Eq. (14)) generates a dissipative power $-I\Delta\mu \equiv I(\mu_s - \mu_d) \geq 0$ in each channel that has to be dissipated into the reservoirs, and the total amount of heat flow \dot{Q} into the reservoirs thus is

$$\dot{Q} \equiv -NI\Delta\mu - \frac{d}{dt} \langle E(\mathbf{n}) \rangle_t. \quad (32)$$

We note that this simple splitting of \dot{Q} into two contributions is a consequence of our model for the rates Eq. (10), with its separation of excitation energies $\varepsilon_l(\mathbf{n}) \equiv \Delta\mu_l + \Delta E_l(\mathbf{n})$ into a constant single particle part $\Delta\mu_l$ and the part $\Delta E_l(\mathbf{n})$ with the interaction energies Eq. (9).

In the following, we check Eq. (32) by a somewhat more elaborate argument based on entropy.

C. Fokker–Planck equation

We use an approximation to the original rate equations Eq. (2) where the integers n_l become continuous, real number x_l of which only Gaussian fluctuations are kept. In this way, we obtain a Fokker–Planck equation for the probability distribution $P(\mathbf{x}, t)$ in the usual form of a continuity equation

$$\frac{\partial}{\partial t} P(\mathbf{x}, t) = - \sum_{l=1}^N \frac{\partial}{\partial x_l} J_l(\mathbf{x}, t) \quad (33)$$

$$J_l(\mathbf{x}, t) \equiv F_l(\mathbf{x})P(\mathbf{x}, t) - \frac{\gamma}{2} \frac{\partial}{\partial x_l} P(\mathbf{x}, t), \quad (34)$$

with diffusion constant $\frac{\gamma}{2}$ and force term $F_l(\mathbf{x}) \equiv \gamma_+ - \gamma_- + \sum_{j=1}^N g_{lj}(x_j - x_l)$.

Since $F_l(\mathbf{x})$ is linear, this can be solved exactly and thus be used to derive explicit expressions for the Shannon entropy

$$S(t) \equiv -\langle \ln P \rangle_t \equiv - \int d\mathbf{x} P(\mathbf{x}, t) \ln P(\mathbf{x}, t). \quad (35)$$

Moreover, Eq. (33) is very convenient for directly reading off the splitting of the temporal change,

$$\frac{d}{dt} S(t) = \Pi(t) - \Phi(t), \quad (36)$$

into a (positive) entropy production rate $\Pi(t)$ and the global entropy flow

$$\Phi(t) \equiv \sum_{l=1}^N \left\langle \frac{2}{\gamma} F_l^2(\mathbf{x}) + \frac{\partial F_l(\mathbf{x})}{\partial x_l} \right\rangle_t \quad (37)$$

from the total system into the reservoirs [43]. Crucially, even though $S(t)$ and $\Pi(t)$ are ‘abstract’ quantities in the sense that they are no direct experimental observables, the entropy flow $\Phi(t)$ directly yields the (measurable) heat flow $\dot{Q} \equiv \frac{1}{\beta} \Phi(t)$ into the reservoirs. The expectation value Eq. (37) can be expressed in terms of the second cumulants $\langle \delta x_l \delta x_{l'} \rangle$ via the identification $n_l \leftrightarrow x_l$ from the $C_{ll'}(t)$, Eq. (15), or from the direct solution of Eq. (33) (see below). Using Fourier transformation and some straightforward algebra, one obtains

$$\dot{Q} \equiv \frac{1}{\beta} \Phi(t) = -\frac{2NI}{\beta} \tanh \frac{\beta\Delta\mu}{2} - \frac{d}{dt} \langle E(\mathbf{n}) \rangle_t. \quad (38)$$

Now recalling that in the derivation of our classical transitions rates after Eq. (8) we demanded $\beta|\Delta\mu| \ll 1$, we may replace the \tanh in Eq. (38) by its argument and thus recover our previous result Eq. (32) that was based upon a simple energy argument.

D. Feedback information flow

Finally, we quantify the information flow in the ‘feedback-freezing’ of the distribution $P(\mathbf{x}, t)$. Eq. (33)

models the continuous counting variables x_l as the positions of N linearly coupled Brownian particles, a situation analysed in detail (for $N = 2$) by Allahverdyan *et al.* [44] via the mutual information \mathcal{I} . Recently, Horowitz [26] has generalized this to multipartite systems governed by Fokker–Planck equations like Eq. (33) and introduced an information flow based on the concept of neighbours influencing each other.

Here, we use the simplest bipartite splitting of the whole system into a single channel $l = 1$ (with probability density $P_1(x_1, t)$) and the remaining $N - 1$ channels (with probability density $P_{1'}(x_2, \dots, x_n, t)$), where the mutual information

$$\mathcal{I}(t) \equiv \int d^N \mathbf{x} P(\mathbf{x}, t) \ln \frac{P(\mathbf{x}, t)}{P_1(x_1, t) P_{1'}(x_2, \dots, x_n, t)} \quad (39)$$

quantifies the build-up of feedback effects within a small subsystem (single channel) embedded into a large feedback environment.

The temporal change $\dot{\mathcal{I}}(t) = \iota_{1' \rightarrow 1} + \iota_{1 \rightarrow 1'}$ defines the two information flows between the two subsystems [21, 44]. Using Eq. (33) and the equivalence of all channels, we can express the flows via entropies [44], such as

$$\iota_{1' \rightarrow 1}(t) = \dot{S}_1(t) - \frac{1}{N} \dot{S}(t), \quad (40)$$

with the Shannon entropy $S(t)$ of the total system, Eq. (35), and the quantity

$$\dot{S}_1(t) \equiv \int d^N \mathbf{x} \left(\frac{\partial}{\partial x_1} J_1(\mathbf{x}, t) \right) \ln P_1(x_1, t) \quad (41)$$

which has the form of a *local* Shannon entropy change, cf. Appendix C.

In \mathbf{k} -space, we find that the second cumulants $\sigma_{\mathbf{k}}(t)$ (defined in Eq. (19)) completely determine the entropies via

$$\dot{S}_1(t) = \frac{1}{2} \frac{d}{dt} \ln \sum_{\mathbf{k}} \sigma_{\mathbf{k}}(t), \quad \dot{S}(t) = \frac{1}{2} \frac{d}{dt} \sum_{\mathbf{k}} \ln \sigma_{\mathbf{k}}(t), \quad (42)$$

which in view of our Gaussian approximation is not so surprising, but demonstrates that there is a direct connection between the (abstract) information flow Eq. (40) and a fluctuation quantity that at least in principle is accessible via the counting statistics. This argument is in line with recent results by Ansari and Nazarov [45], who derived a general connection between Renyi (and Shannon) entropy and full counting statistics.

At small times t , owing to $\sigma_{\mathbf{k}}(t \rightarrow 0) \approx \gamma t$, the information flow is zero although both entropy changes are large, $\dot{S}_1(t) = \frac{1}{N} \dot{S}(t) \approx \frac{1}{2t}$, the latter being due to the initial condition $P(\mathbf{x}, t = 0) = \delta^N(\mathbf{x})$. On the other hand, at any finite N and large times t , only the $\mathbf{k} = 0$ component significantly contributes to Eq. (42) since $\sigma_{\mathbf{k}}(t \rightarrow \infty) \approx \delta_{\mathbf{k}, 0} \gamma t$ and the information flow decays towards zero again, $\iota_{1' \rightarrow 1}(t \rightarrow \infty) \sim \frac{1}{t}$.

In its transient dynamics, thus, $\iota_{1' \rightarrow 1}(t)$ has a maximum at some finite time of the order $g\gamma$, where g is the

dimensionless coupling constant of the interaction model. This behavior is shown in Fig. (2).

For the infinite-range interaction model Eq. (20), the difference between local and total Shannon entropy vanishes with increasing N since the notion of ‘boundary’ between subsystems becomes meaningless. Accordingly, with $\dot{S}_1(t) = \frac{1}{N} \dot{S}(t) = g(e^{-2g\gamma t} - 1)^{-1}$ for $N \rightarrow \infty$, the information flow vanishes. On the other hand, at large but finite N , an interesting feature then is the plateau in $\iota_{1' \rightarrow 1}(t)$ at intermediate times, which is shown in the lower part of Fig. (2) and which clearly corresponds to the ‘freezing’ of the fluctuations, i.e. the plateau in the second cumulants $C_{II}(t)$.

V. DISCUSSION

The autonomous feedback control discussed here is based on a microscopic mechanism, but it comes with the constraints Eq. (11) and Eq. (12) for the interactions U_{lj} , which suggests uncharged particles as appropriate candidates, such as ultracold atoms used in recent transport experiments [46]. In contrast, for charged particles (e.g., for electronic transport), the non-autonomous, synchronization feedback model Eq. (3) (which essentially is an open-loop control scheme in the space of particle numbers n), appears to be more flexible.

Needless to say that the choice of a particular control scheme depends on the specific control task, which in our model was to stabilize the full counting statistics at a given particle current $I = \gamma_+ - \gamma_-$ over a longer time t . One aspect then is the issue of energy cost and efficiency. The two control schemes mentioned above both scale linearly in t in terms of energy costs: the non-autonomous scheme by requiring a continuing modulation of energy barriers, and the autonomous scheme by needing large channel numbers $N \propto t$ (and thus a large total heat flow $\frac{1}{2} k_B T N \propto t$, cf. after Eq. (31)) if stabilization over large intervals t is required, as we saw in Fig. (2a).

The analysis proposed here remained at the level of a Gaussian approximation for the full counting statistics, i.e. a linear Fokker-Planck equation. Our results might stimulate further work to explore the connection between the recently discussed flow of information in feedback networks [21, 22, 26, 36], and the dynamical scaling type analysis for transport processes in interacting systems, such as in the Kardar-Parisi-Zhang (KPZ) model [39] for particle deposition and surface growth. For this latter point, the most urgent step then is to go beyond the linear (in \mathbf{n}) approximation Eq. (10) of the rates, either by going to higher orders in the expansion Eq. (7) (i.e., beyond the classical limit and towards lower temperatures), or by sticking to the classical limit Eq. (7) and employing interaction models beyond the simple quadratic model Eq. (9). An interesting alternative there could be the study of the KPZ equation (or other Langevin equations belonging to Eq. (2)) *per se* from the perspective of entropy and information flow.

Acknowledgements

I thank M. Esposito, G. Schaller and P. Strasberg for valuable discussions, and I acknowledge support by the DFG via projects BR 1528/7-1, 1528/8-1, 1528/9-1, SFB 910 and GRK 1558.

Appendix A: Non-autonomous feedback in single-channel model

Here, we derive the equation of motion for the reduced probability

$$p_1(n, t) \equiv \sum_{\mathbf{n}} \delta_{n_1, n} p(\mathbf{n}, t), \quad (\text{A1})$$

with $\mathbf{n} \equiv (n_1, \dots, n_N)^T$, for a single channel (chosen as $l = 1$) in the $N \rightarrow \infty$ limit of the constant interaction model in Eq. (20). After multiplying Eq. (2) with $\delta_{n_1, n}$ and summing over \mathbf{n} , only the $l = 1$ term of the sum over l remains and

$$\begin{aligned} \dot{p}_1(n, t) &= \sum_{\mathbf{n}, \pm} \delta_{n_1, n} [\gamma_{1\mp}(\mathbf{n} \pm \mathbf{e}_1) p(\mathbf{n} \pm \mathbf{e}_1, t) - \gamma_{1\mp}(\mathbf{n}) p(\mathbf{n}, t)]. \end{aligned} \quad (\text{A2})$$

For $g_{ij} = \frac{g}{N}$, the rates have the form $\gamma_{1\pm}(\mathbf{n}) = f_{\pm}(n_{\text{av}} - n_1)$, with the average $n_{\text{av}} \equiv (n_1 + \dots + n_N)/N$ and $f_{\pm}(x) = \gamma_{\pm}(1 \pm gx)$ for the linear rate model Eq. (5) with feedback parameter g . Now, for $N \rightarrow \infty$ the average n_{av} becomes a macroscopic variable. We neglect the fluctuations of the latter against those of n_1 by factorizing

$$\begin{aligned} \sum_{\mathbf{n}} \delta_{n_1, n} \gamma_{1\mp}(\mathbf{n}) p(\mathbf{n}, t) &= \sum_{\mathbf{n}} \delta_{n_1, n} f_{\mp}(n_{\text{av}} - n) p(\mathbf{n}, t) \\ &\approx f_{\mp}(\langle n_{\text{av}} \rangle_t - n) p_1(n, t) \end{aligned} \quad (\text{A3})$$

and similar for the terms $\gamma_{1\mp}(\mathbf{n} \pm \mathbf{e}_1) p(\mathbf{n} \pm \mathbf{e}_1, t)$ in Eq. (A2). In this approximation, we effectively neglect the backaction of the first channel on all the other $N - 1$ channels.

In this mean-field type approach, the effect of the other channels is that of an external ‘clock’ as expressed by the time-dependence of $\langle n_{\text{av}} \rangle_t = (\gamma_+ - \gamma_-)t \equiv It$ according to Eq. (14). This leads to

$$\begin{aligned} \dot{p}_1(n, t) &= \sum_{\pm} [f_{\mp}(It - n \mp 1) p_1(n \pm 1, t) \\ &\quad - f_{\mp}(It - n) p_1(n, t)], \end{aligned} \quad (\text{A4})$$

which describes non-autonomous feedback control as in [34] via rates Eq. (3) with the ‘control current’ $I = \gamma_+ - \gamma_-$. As mentioned already after Eq. (21), the second cumulant Eq. (4) of the model Eq. (A4) co-incides with that of the constant interaction N -channel model, Eq. (21), for $N \rightarrow \infty$. In that limit and within the Gaussian approximation, the correspondence therefore is exact.

Appendix B: Noise Spectrum

The symmetrized noise spectrum $S_{ll'}(\omega)$, Eq. (25), follows from the MacDonald formula as outlined, e.g., in [41]. One starts from

$$S_{ll'}(\omega) = \int_{-\infty}^{\infty} d\tau e^{i\omega\tau} \langle \delta I_l(t + \tau) \delta I_{l'}(t) + (l \leftrightarrow l') \rangle, \quad (\text{B1})$$

which still depends on the initial time t that is sent to infinity at the end. We write

$$\int_t^{t+\tau} dt' \delta I_l(t') = \delta n_l(t + \tau) - \delta n_l(t), \quad (\text{B2})$$

where $\delta n_l(t) \equiv n_l(t) - tI_l$ with $tI_l = \langle n_l(t) \rangle$, cf. Eq. (14). As in [41], this leads to

$$\begin{aligned} \frac{S_{ll'}(\omega)}{2\omega} &= \int_0^{\infty} d\tau \sin(\omega\tau) \\ &\times \frac{\partial}{\partial \tau} \langle [\delta n_l(t + \tau) - \delta n_l(t)] [\delta n_{l'}(t + \tau) - \delta n_{l'}(t)] \rangle. \end{aligned} \quad (\text{B3})$$

To proceed, we now need (in the mixed terms in Eq. (B3)) the two-time correlation functions $\langle \delta n_l(t) \delta n_{l'}(t + \tau) \rangle$, which in view of Eq. (13) fulfill the regression equations

$$\begin{aligned} \frac{d}{d\tau} \langle \delta n_l(t) \delta n_{l'}(t + \tau) \rangle &= \\ &= \gamma \sum_{j=1}^N g_{l'j} (\langle \delta n_l(t) \delta n_j(t + \tau) \rangle - (j \rightarrow l')). \end{aligned} \quad (\text{B4})$$

We can solve this by first transforming into Fourier (\mathbf{k}) space similar to what we did to obtain the equal time correlation function $C_{ll'}(t) = \langle \delta n_l(t) \delta n_{l'}(t) \rangle$ in Eq. (18), which in fact serves as the initial condition at $\tau = 0$ here. The result

$$\begin{aligned} \langle \delta n_l(t) \delta n_{l'}(t + \tau) \rangle &= \\ \frac{\gamma t}{N} + \frac{\gamma}{N} \sum_{\mathbf{k} \neq 0} \frac{e^{-i\mathbf{k}(\mathbf{R}_l - \mathbf{R}_{l'})}}{\Gamma_{\mathbf{k}}} (1 - e^{-\Gamma_{\mathbf{k}} t}) e^{-\frac{\Gamma_{\mathbf{k}}}{2} \tau} \end{aligned} \quad (\text{B5})$$

can now be used in the MacDonald formula Eq. (B3), leading to

$$\begin{aligned} S_{ll'}(\omega) &= 2\omega \int_0^{\infty} d\tau \sin(\omega\tau) \\ &\times \left[\frac{\gamma}{N} + \frac{\gamma}{N} \sum_{\mathbf{k} \neq 0} \cos(\mathbf{k}(\mathbf{R}_l - \mathbf{R}_{l'})) e^{-\frac{\Gamma_{\mathbf{k}}}{2} \tau} \right]. \end{aligned} \quad (\text{B7})$$

Here, as usual [41] the sine function under the integral in the first term has to be understood as the limit $\sin \omega\tau = \lim_{\eta \rightarrow 0} \Im e^{i(\omega - \eta)\tau}$, and we now obtain Eq. (26).

Appendix C: Information flow

From Eq. (39), the temporal change of the mutual information $\mathcal{I}(t)$ is

$$\dot{\mathcal{I}}(t) = - \sum_{l=1}^N \frac{\partial}{\partial x_l} J_l(\mathbf{x}, t) [\ln P - \ln P_1 - \ln P_{1'}], \quad (\text{C1})$$

where we used Eq. (33) and the conservation of probabilities, $\int dx_1 \dot{P}_1(x_1, t) = 0$, $\int dx_2 \dots dx_N \dot{P}_{1'}(x_2, \dots, x_N, t) = 0$, $\int d^N \mathbf{x} \dot{P}(\mathbf{x}, t) = 0$. We can write

$$\begin{aligned} & \int d^N \mathbf{x} \left(\frac{\partial}{\partial x_1} J_1(\mathbf{x}, t) + \sum_{l=2}^N \frac{\partial}{\partial x_l} J_l(\mathbf{x}, t) \right) \ln P_1(x_1, t) \\ &= \int d^N \mathbf{x} \left(\frac{\partial}{\partial x_1} J_1(\mathbf{x}, t) \right) \ln P_1(x_1, t) \end{aligned} \quad (\text{C2})$$

by integration of parts of the second term, and similar for $\ln P_{1'}$. This yields the splitting $\dot{\mathcal{I}}(t) \equiv \iota_{1' \rightarrow 1} + \iota_{1 \rightarrow 1'}$ with the information flows

$$\begin{aligned} \iota_{1' \rightarrow 1} &\equiv - \int d^N \mathbf{x} \left(\frac{\partial}{\partial x_1} J_1(\mathbf{x}, t) \right) \ln \frac{P}{P_1} \\ \iota_{1 \rightarrow 1'} &\equiv - \int d^N \mathbf{x} \left(\sum_{l=2}^N \frac{\partial}{\partial x_l} J_l(\mathbf{x}, t) \right) \ln \frac{P}{P_{1'}}. \end{aligned} \quad (\text{C3})$$

Using the definitions of the global and local Shannon entropies, Eq. (35) and Eq. (41), we can now write the information flow $\iota_{1' \rightarrow 1}$ from channels 2, ..., N to channel 1 in the form Eq. (40).

For the evaluation of $\frac{d}{dt} S_1(t)$, Eq. (41), we use integration by parts to write

$$\frac{d}{dt} S_1(t) = - \left\langle F_1(\mathbf{x}) \frac{\partial}{\partial x_1} P_1 \right\rangle - \frac{\gamma}{2} \left\langle \frac{\partial}{\partial x_1} \frac{\partial}{\partial x_1} P_1 \right\rangle \quad (\text{C4})$$

We use the fact that $P_1(x_1, t)$ has to be a Gaussian, and we thus obtain (with the definition of $F_1(\mathbf{x})$ in Eq. (33)) the explicit form

$$\begin{aligned} \frac{d}{dt} S_1(t) &= \frac{1}{\langle \delta x_1^2 \rangle} \sum_{j=1}^N g_{1j} \langle (\delta x_j - \delta x_1) \delta x_1 \rangle + \frac{\gamma}{2 \langle \delta x_1^2 \rangle} \\ &= \gamma \frac{\sum_{\mathbf{k}} e^{-\Gamma_{\mathbf{k}} t}}{2 \sum_{\mathbf{k}} \sigma_{\mathbf{k}}} = \frac{1}{2} \frac{d}{dt} \ln \sum_{\mathbf{k}} \sigma_{\mathbf{k}}(t), \end{aligned} \quad (\text{C5})$$

where $\delta x_1 = x_1 - (\gamma_+ - \gamma_-)t$ and we used Fourier components, $\langle \delta x_1^2 \rangle = \frac{1}{N} \sum_{\mathbf{k}} \sigma_{\mathbf{k}}$, and the second cumulants $\sigma_{\mathbf{k}}(t)$ in \mathbf{k} space, Eq. (19).

For the global Shannon entropy change, in a similar manner (by exploiting the equivalence of all channels l in the homogeneous case) we obtain

$$\begin{aligned} \frac{1}{N} \frac{d}{dt} S(t) &= \int d^N \mathbf{x} \frac{\partial}{\partial x_1} J_1(\mathbf{x}, t) \ln P(\mathbf{x}, t) \\ &= \frac{1}{2N} \sum_{\mathbf{k}} \frac{\Gamma_{\mathbf{k}} e^{-\Gamma_{\mathbf{k}} t}}{1 - e^{-\Gamma_{\mathbf{k}} t}} = \frac{1}{2N} \frac{d}{dt} \sum_{\mathbf{k}} \ln \sigma_{\mathbf{k}}(t), \end{aligned} \quad (\text{C6})$$

where again we used the fact that the full distribution function P is a Gaussian.

-
- [1] J. Zhang, Y. Liu, R. Wu, K. Jacobs, F. Nori, arXiv:1407.8536 [quant-ph] (2014).
- [2] H. M. Wiseman and G. J. Milburn, *Quantum Measurement and Control* (Cambridge University Press, Cambridge, England, 2009).
- [3] S. Toyabe, T. Sagawa, M. Ueda, E. Muneyuki, and M. Sano, Nat. Phys. **6**, 988 (2010).
- [4] G. Schaller, C. Emary, G. Kießlich, and T. Brandes, Phys. Rev. B **84**, 085418 (2011).
- [5] D. V. Averin, M. Möttönen, and J. P. Pekola, Phys. Rev. B **84**, 245448 (2011).
- [6] D. Abreu and U. Seifert, Europhys. Lett. **94**, 10001 (2011).
- [7] Y. Jun and J. Bechhoefer, Phys. Rev. E **86**, 061106 (2012).
- [8] J. Bergli, Y. M. Galperin, and N. B. Kopnin, Phys. Rev. E **88**, 062139 (2013).
- [9] J. V. Koskia, V. F. Maisia, J. P. Pekola, and D. V. Averin, PNAS **111** (38), 13786 (2014).
- [10] S. A. M. Loos, R. Gernert, and S. H. L. Klapp, Phys. Rev. E **89**, 5 (2014).
- [11] T. Sagawa and M. Ueda, Phys. Rev. Lett. **100**, 080403 (2008).
- [12] T. Sagawa and M. Ueda, Phys. Rev. Lett. **104**, 090602 (2010).
- [13] J. Horowitz and J. M. P. Parrondo, Europhys. Lett. **95**, 10005 (2011).
- [14] T. Sagawa and M. Ueda, Phys. Rev. E **85**, 021104 (2012).
- [15] D. Abreu and U. Seifert, Phys. Rev. Lett. **108**, 030601 (2012).
- [16] T. Munakata and M. L. Rosinberg, J. Stat.Mech. (2012) P05010.
- [17] M. Esposito and G. Schaller, Europhys. Lett. **99**, 30003 (2012).
- [18] J. M. Horowitz, T. Sagawa, and J. M. R. Parrondo, Phys. Rev. Lett. **111**, 010602 (2013).
- [19] P. Strasberg, G. Schaller, T. Brandes, and M. Esposito, Phys. Rev. Lett. **110**, 040601 (2013).
- [20] H. Tasaki, arXiv:1308.3776 (2013).
- [21] J. M. Horowitz, M. Esposito, Phys. Rev. X **4**, 031015 (2014).
- [22] D. Hartich, A. C. Barato, U. Seifert, J. Stat. Mech. P02016 (2014).
- [23] A.C. Barato and U. Seifert, Phys. Rev. Lett. **112**, 090601 (2014).
- [24] N. Shiraiishi and T. Sagawa, Phys. Rev. E **91**, 012130 (2015).
- [25] P. Strasberg, G. Schaller, T. Brandes, and C. Jarzynski,

- Phys. Rev. E **90**, 062107 (2014).
- [26] J. M. Horowitz, arXiv:1501.05549 (2015).
- [27] A. L. Grimsmo, arXiv:1502.06959 (2015).
- [28] S. Lloyd, Phys. Rev. A **62**, 022108 (2000).
- [29] A. Carmele, J. Kabuss, F. Schulze, S. Reitzenstein, and A. Knorr, Phys. Rev. Lett. **110**, 013601 (2013).
- [30] S. M. Hein, F. Schulze, A. Carmele, and A. Knorr, Phys. Rev. Lett. **113**, 027401 (2014).
- [31] A. L. Grimsmo, A. S. Parkins, and B.-S. Skagerstam, New J. Phys. **16**, 065004 (2014).
- [32] W. Kopylov, C. Emary, E. Schöll, T. Brandes, New J. Phys. **17**, 013040 (2015).
- [33] C. Emary and J. Gough, Phys. Rev. B **90**, 205436 (2014).
- [34] T. Brandes, Phys. Rev. Lett. **105**, 060602 (2010).
- [35] *Quantum Noise in Mesoscopic Physics*, edited by Y. V. Nazarov (Kluwer Academic, Dordrecht, 2003), Vol. 97.
- [36] S. Ito, T. Sagawa, Phys. Rev. Lett. **111**, 180603 (2013).
- [37] H. Bruus and K. Flensberg, *Many-Body Quantum Theory in Condensed Matter Physics*, Oxford University Press (2004).
- [38] P. C. Hohenberg and B. I. Halperin, Rev. Mod. Phys. **49**, 435 (1977).
- [39] M. Kardar, *Statistical Physics of Fields*, Cambridge University Press (2007).
- [40] D. K. C. MacDonald, Rep. Prog. Phys. **12**, 56 (1948).
- [41] N. Lambert, R. Aguado, and T. Brandes, Phys. Rev. B **75**, 045340 (2007).
- [42] H. L. Carmichael, *Statistical Methods in Quantum Optics I*, Springer, Berlin (2002).
- [43] T. Tomé, Braz. J. Phys. **36**, 1285 (2006).
- [44] A. E. Allahverdyan, D. Janzing, G. Mahler, J. Stat. Mech. P09011 (2009).
- [45] M. H. Ansari and Y. V. Nazarov, arXiv:1502.08020 (2015).
- [46] S. Krinner, D. Stadler, D. Husmann, J.-P. Brantut, and T. Esslinger, Nature **517**, 64 (2015).